

### Nucleus-nucleus total reaction cross sections

R. M. DeVries and J. C. Peng

Los Alamos Scientific Laboratory, Los Alamos, New Mexico 87545

(Received 13 November 1979)

We compare  $\sigma_R(E)$  for nucleus-nucleus systems (obtained from existing direct measurements and derived from elastic scattering data) with nucleon-nucleon and nucleon-nucleus data. The energy dependence of  $\sigma_R(E)$  for nucleus-nucleus systems is found to be quite rapid; there appears to be no evidence for an energy independent, geometric  $\sigma_R$ . Simple parameter free microscopic calculations are able to quantitatively reproduce the data and thus, emphasize the dominance of nucleon-nucleon interactions in medium energy nucleus-nucleus collisions.

NUCLEAR REACTIONS Total reaction cross section theory, comparison to data for  $d, {}^3\text{He}, \alpha + {}^{12}\text{C}, {}^{40}\text{Ca}, {}^{90}\text{Zr}, {}^{208}\text{Pb}$  and  ${}^{12}\text{C} + {}^{12}\text{C}$ . Predictions for  ${}^{40}\text{Ca} + {}^{40}\text{Ca}, {}^{40}\text{Ca} + {}^{208}\text{Pb}, {}^{208}\text{Pb} + {}^{208}\text{Pb}$ . Energy range  $3 < E_i/n < 1000$  MeV.

#### I. INTRODUCTION

Medium and high energy heavy-ion beams are beginning to become available to experimentalists. It is important to understand the basic gross features of nucleus-nucleus ( $\mathcal{N}$ - $\mathcal{N}$ ) collisions, e.g., elastic scattering and total reaction cross sections ( $\sigma_R$ ). It is commonly assumed that  $\sigma_R(E)$  for  $\mathcal{N}$ - $\mathcal{N}$  collisions is constant and equal to the geometric limit at medium energies. In this paper we address the question of  $\sigma_R(E)$  for  $\mathcal{N}$ - $\mathcal{N}$  collisions on the basis of experimental data and basic theoretical considerations.

We start illustrating by and discussing nucleon-nucleon ( $N$ - $N$ ) and nucleon-nucleus ( $N$ - $\mathcal{N}$ ) systems. The basic behavior of these systems is found to extend to the  $\mathcal{N}$ - $\mathcal{N}$  case. Therefore, microscopic calculations based on  $\sigma_T^{NN}(E)$  seem to be called for. Specifically the optical limit of Glauber theory is applied. We show that such calculations are capable of quantitatively reproducing all of the available data. This agreement strongly emphasizes the dominance of the  $N$ - $N$  interaction for  $\mathcal{N}$ - $\mathcal{N}$  collisions at medium energies.

#### II. NUCLEON-NUCLEON AND NUCLEON-NUCLEUS SYSTEM

The behavior of the  $N$ - $N$  total cross section ( $\sigma_T^{NN}$ ) is well known. Figure 1 displays  $\sigma_T^{NN}(E)$  for incident (laboratory) energies up to 1 GeV.<sup>1</sup> Notice the rapid decrease in  $\sigma_T^{NN}$  with increasing energy up to about 300 MeV at which point  $\pi$  production causes the cross section to rise. This pronounced dip in  $\sigma_T^{NN}(E)$  can be traced to the behavior of the scattering phase shifts (in particular, the  ${}^1S_0$  phase shift crosses zero in the region of the dip). The dip should be a characteristic feature of any heavier system which is dominated by the nucleon-nucleon interaction.

Indeed proton-nucleus total reaction cross sections<sup>2</sup> display an energy dependence, which tracks  $\sigma_T^{NN}(E)$  (see Fig. 2) (from Ref. 3). Of course low energy effects due to the Coulomb barrier and resonances are also observed. The fact that  $\sigma_R$  climbs and then levels out in the energy region  $E_i < 20$  MeV suggests that a geometric limit is reached. The fact that  $\sigma_R(E)$  falls off sharply at higher energies means that this geometric limit is not maintained, i.e., some transparency occurs in the nucleon-nucleus interaction at these energies. The data may be parametrized with the formula<sup>2</sup>

$$\sigma_R = \pi(R + \lambda)^2 \left[ 1 - \frac{ZZe^2}{(R + \lambda)E} \right] (1 - T), \quad (1)$$

where  $R$  is the effective nuclear radius,  $\lambda$  is the reduced wave length of the incident particle,  $Z$  and

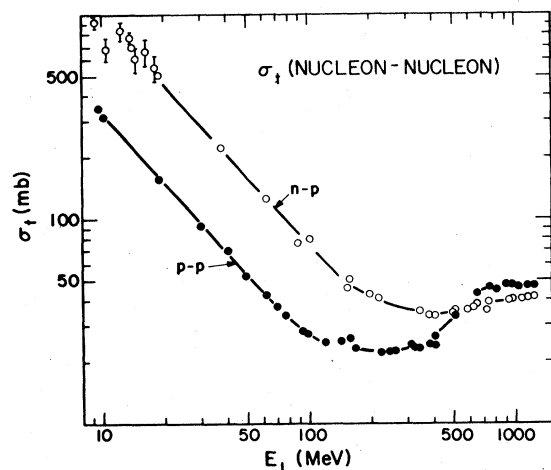


FIG. 1. Nucleon-nucleon total cross sections as a function of incident lab. energy (from Ref. 6).

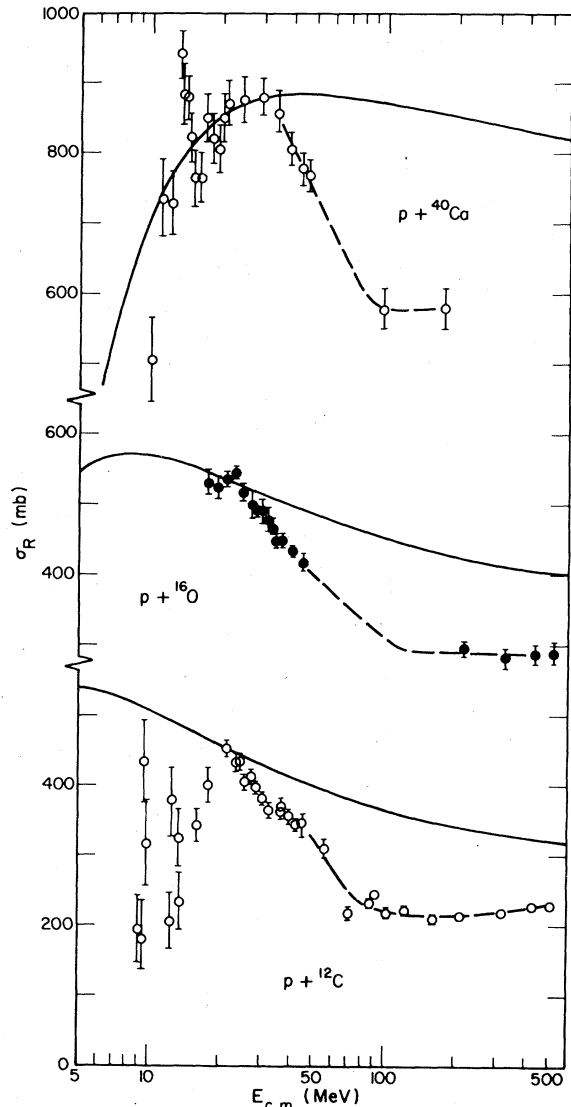


FIG. 2. Examples of proton  $\sigma_R(E)$  (from Ref. 3). The dashed lines are drawn to guide the eye and the solid lines are fits using Eq. (1) with  $T=0$ . The parameters of these fits are listed in Table I.

$z$  refer to the target and projectile, respectively,  $E$  is the center-of-mass energy, and  $T$  is the transparency, which may be related to the mean-free path of the nucleon in nuclear matter. Thus transparency as defined in this equation represents the difference between the geometric cross section and the experimentally smaller values which are obtained at intermediate energies. This transparency is apparently related to the behavior of  $\sigma_T^{NN}(E)$ . (Microscopic theoretical calculations of  $\sigma_R^{NN}$  will be presented in Sec. IV.)

Figure 2 shows the application of Eq. (1) to existing proton  $\sigma_R$  data. The radius in Eq. (1) is determined by fitting the low energy data (with

$T=0$ ). Equation (1) is then extrapolated to the medium energy region. This  $T=0$  prediction, as shown in Fig. 2, definitely overestimates the medium energy data, hence a nonzero value of  $T$  is required to describe the medium energy data. The derived radii and  $T$  values are listed in Table I. The derived radii are fairly close to electron scattering radii which seems to justify the assumption that  $T=0$  at the peak of  $\sigma_R(E)$ . The derived values of  $T$  are in reasonable accord with the work of Renberg *et al.*<sup>2</sup>

### III. NUCLEUS-NUCLEUS SYSTEMS

Very little  $\sigma_R(E)$  data have been measured for  $\mathcal{N}$ - $\mathcal{N}$  systems. However, the fact that composite projectiles and heavy ions are known to be strongly absorbed (at low incident energies) has encouraged the assumption that  $\sigma_R(E)$  simply levels off, above the Coulomb barrier, at the geometric limit and stays at that value at intermediate and high incident energies.

As we shall see, elastic scattering data are very useful in studying the energy dependence of the  $\mathcal{N}$ - $\mathcal{N}$  interaction. It is well established that elastic scattering data can be reasonably well described with a diffraction model<sup>4</sup> in which the minima of the angular distribution are given by the zeros of  $J_1^2(kR\theta)$ . We have compared  $\alpha + {}^{40}\text{Ca}$  data with this diffraction model at  $E_{c.m.}/N$  (i. e., the center of mass energy divided by the number of nucleons in the projectile) = 32.2 (Ref. 5) and 306.7 MeV (Ref. 6) incident energies. At both energies the first four minima are closely reproduced with this description. However, the radius required to fit the data changes from 6.40 fm at 32.2 MeV/ $N$  to about 4.9 fm at 306.7 MeV/ $N$ . This simple analysis suggests that the geometry seen in composite projectile-nucleus collisions changes as a function of incident energy. Thus the value of the geometrical limit for  $\sigma_R$  may be quite different between these two energies.

Quantitatively,  $\sigma_R$  may be deduced from elastic scattering data using the optical model. The consistency between direct (e. g., beam attenuation) and elastic scattering-optical model values of  $\sigma_R$  to the level of a few percent is well established for low and medium energy  $N$ - $\mathcal{N}$  systems. We have verified this agreement for proton-nucleus scattering at energies up to 1 GeV by comparing direct attenuation  $\sigma_R$  measurements with values deduced from elastic scattering.

The equivalence between the two techniques has also been shown to hold for composite projectiles at low energies.<sup>7</sup> A comparison at medium energies seems to be possible for only one system ( $d + {}^{12}\text{C}$ ), since so few direct measurements have

TABLE I. Parameters used in Eq. (1).

Analysis parameters				
System	Radius in Eq. (1)(fm)	Electron scattering radius <sup>a</sup> (fm)	$T$ (in minimum)	Geometric $\sigma_R$ (mb) <sup>b</sup>
$p + {}^{12}\text{C}$	2.98	3.16	36%	314
$p + {}^{16}\text{O}$	3.39	3.49	32%	382
$p + {}^{40}\text{Ca}$	4.95	4.45	32%	623
$d + {}^{12}\text{C}$	5.45	5.87	64%	1082
${}^3\text{He} + {}^{12}\text{C}$	5.70	5.58		977
$\alpha + {}^{12}\text{C}$	5.10	5.36	54%	902
$d + {}^{40}\text{Ca}$	6.85	7.16		1610
${}^3\text{He} + {}^{40}\text{Ca}$	7.50	6.87		1482
$\alpha + {}^{40}\text{Ca}$	7.00	6.65	40%	1389
$d + {}^{90}\text{Zr}$	8.70	8.22		2121
${}^3\text{He} + {}^{90}\text{Zr}$	9.00	7.93		1974
$\alpha + {}^{90}\text{Zr}$	8.50	7.71		1866
$d + {}^{208}\text{Pb}$	10.6	9.81	38%	3020
$\alpha + {}^{208}\text{Pb}$	10.6	9.30		2714
${}^{12}\text{C} + {}^{12}\text{C}$	6.82	6.33	36%	1257
${}^{40}\text{Ca} + {}^{40}\text{Ca}$		8.91		2493
${}^{40}\text{Ca} + {}^{208}\text{Pb}$		11.55		4194
${}^{208}\text{Pb} + {}^{208}\text{Pb}$		14.20		6336

<sup>a</sup>  $(\frac{5}{3})^{1/2}$  times  $R_{\text{rms}}$  (from Ref. 11).  $R_{\text{rms}}$  is the sum of the projectile and target radius except for the proton systems where only the target size is included.

<sup>b</sup>  $\pi R^2$  where  $R$  is from column 3.

been performed for  $\pi$ - $\pi$  systems. Figure 3 displays  $\sigma_R(E)$  for  $d + {}^{12}\text{C}$ , derived from elastic scattering data,<sup>8</sup> along with three direct (beam attenuation measurements).<sup>9,10</sup> The overall agreement is reasonably clear and suggests that elastic scattering data can be used to obtain  $\pi$ - $\pi$   $\sigma_R$  values to an accuracy of about  $\pm 5\%$ .

Figure 3 also displays  $\sigma_R(E)$  data for the  $p + {}^{12}\text{C}$  system, which can be compared with the  $d + {}^{12}\text{C}$  data. It is very clear that the  $d + {}^{12}\text{C}$  system displays a dramatic energy dependence. If we apply Eq. (1) to the data, normalizing to the large number of data points in the 4–6 MeV/ $N$  region, we obtain the solid curve shown in Fig. 3 and the parameters given in Table I. This curve represents the  $T=0$  (i. e., geometric) limit. Another way of establishing the geometric value for  $\sigma_R$  is to use the electron scattering values<sup>11</sup> for the rms radii to calculate  $\pi(R_d + R_{12\text{C}})^2$  [where  $R = (\frac{5}{3})^{1/2}R_{\text{rms}}$ ]. This technique (see Table I) yields a value of 1082 mb. Thus, the notion that  $\sigma_R$  simply reaches and maintains its geometric limit for  $\pi$ - $\pi$  collisions appears to be completely

incorrect for the  $d + {}^{12}\text{C}$  system.

The  $d + {}^{12}\text{C}$  data set contains a reasonable number of data points; it is impossible to map out  $\sigma_R(E)$  as well for other projectile-target combinations; however, enough data<sup>12</sup> exist to see if the same qualitative effects exist for other cases. Figure 3 also displays data for  ${}^3\text{He}$  and  $\alpha$  projectiles on a  ${}^{12}\text{C}$  target. Data for  $d$ ,  ${}^3\text{He}$ , and  $\alpha$  projectiles are shown in Fig. 4 for a  ${}^{40}\text{Ca}$  target, and in Fig. 5 for a  ${}^{90}\text{Zr}$  target. Figure 6 displays  $d$  and  $\alpha$  data on  ${}^{208}\text{Pb}$  (very little  ${}^3\text{He}$  data exists). Notice that even for  $d + {}^{208}\text{Pb}$ ,  $\sigma_R(E)$  does not stay constant at medium energies.

We apply Eq. (1) to these data to produce the curves shown in Fig. 3 through 6, with parameters given in Table I. The derived radii are in reasonable agreement with the electron scattering values,<sup>11</sup> although there is a tendency for  $R/R_{\text{E.S.}}$  to increase as the mass of the target increases. The values of  $T$  which can be derived from the available medium energy  $\pi$ - $\pi$  data are larger than for the proton data on the same target [e.g.,  ${}^{12}\text{C}$ :  $T_p = 36\%$ ,  $T_d = 64\%$ ,  $T_\alpha = 52\%$ ;  ${}^{208}\text{Pb}$ :  $T_p$ ,

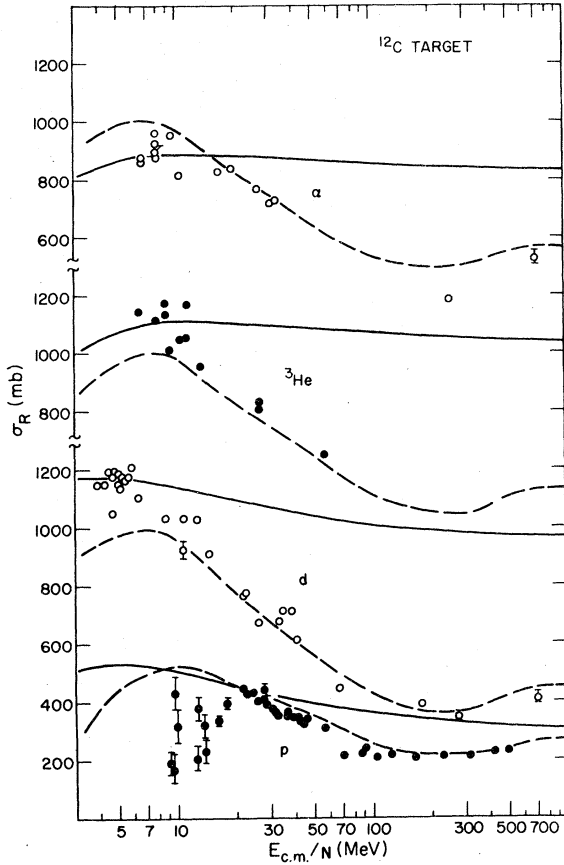


FIG. 3. Total reaction cross section data for a  $^{12}\text{C}$  target. All of the proton points were measured directly. For the  $d$ ,  $^3\text{He}$ , and  $\alpha$  data, the elastic scattering derived values are indicated with no error bars while direct measurements are indicated with error bars. The sources of the data are indicated in the text. The solid lines represent the use of Eq. (1) (with  $T=0$ ) while the dashed lines present the predictions of the microscopic calculations [Eqs. (5) and (6)].

= 10% (Ref. 2),  $T_d=38\%$ ). These larger  $T$  values simply reflect the strong energy dependence found in  $\mathcal{N}$ - $\mathcal{N}$   $\sigma_R(E)$ .

It is interesting to compare the effective radii derived for the three projectiles on a given target. Notice that in all cases ( $^{12}\text{C}$ ,  $^{40}\text{Ca}$ ,  $^{90}\text{Zr}$ ) the effective radius for the  $^3\text{He}$  + target system is larger than for the  $d$  or  $\alpha$  projectiles. Since the  $^3\text{He}$  radius<sup>11</sup> ( $R_{\text{rms}}=1.87$  fm) is intermediate between the  $\alpha$  radius ( $R_{\text{rms}}=1.70$  fm) and the  $d$  radius ( $R_{\text{rms}}=2.1$  fm) we can only conclude that  $\sigma_R$  apparently does *not* scale with projectile radius. Since the differences in  $\sigma_R$  for the three cases are relatively small (compared with the energy dependence, for example) it is particularly important to measure  $\sigma_R(E)$  for these composite projectiles at low incident energies to check this re-

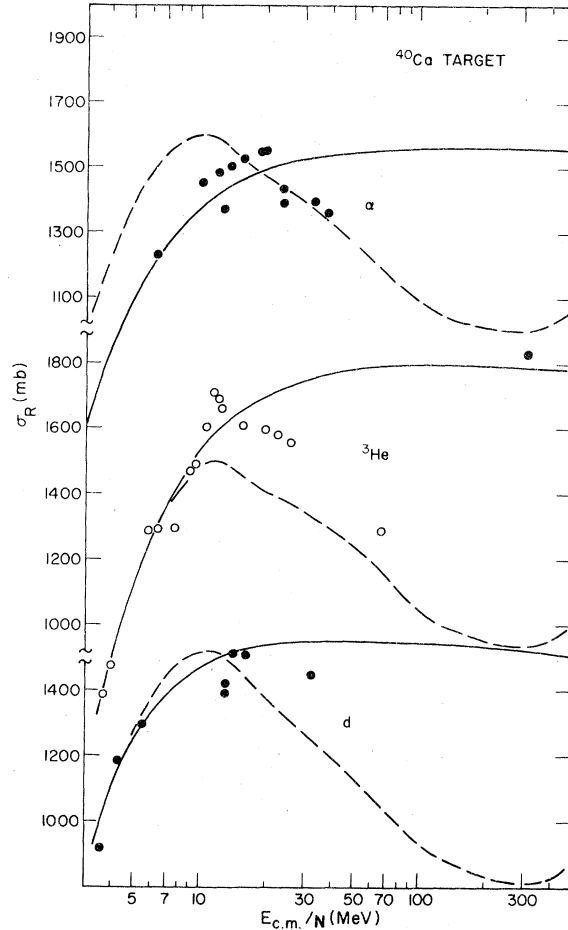


FIG. 4. Total reaction cross sections for a  $^{40}\text{Ca}$  target (see figure caption 4).

sult.

The heaviest system for which data can be gathered is the  $^{12}\text{C} + ^{12}\text{C}$  case. Figure 7 displays elastic scattering based  $\sigma_R$  values<sup>13</sup> at low energy along with two medium energy direct measurements.<sup>10</sup> A curve drawn using Eq. (1) is also shown with parameters listed in Table I.

It is clear that even for  $^{12}\text{C}$  projectiles,  $\sigma_R(E)$  does not simply stay constant at the geometric limit in the medium energy region. As we have seen, this energy dependence can be interpreted as due to an energy dependent radius or transparency. All of these  $\mathcal{N}$ - $\mathcal{N}$  systems appear to display a  $\sigma_R(E)$  behavior strongly reminiscent of  $\sigma_T^{NN}(E)$ . It seems obvious, therefore, to attempt to fit these data with a microscopic model based on  $\sigma_T^{NN}(E)$  as input.

#### IV. MICROSCOPIC CALCULATIONS

We will attempt to fit the  $\sigma_R(E)$  data using the simplest physical concepts. Consider, first of

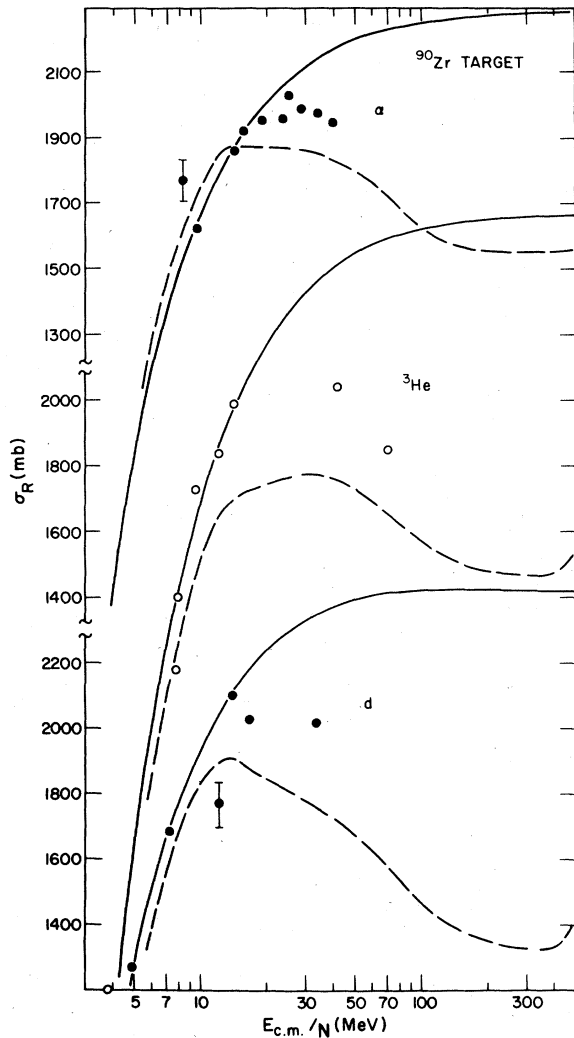


FIG. 5. Total reaction cross sections for a  $^{90}\text{Zr}$  target (see figure caption 4).

all, a chargeless point projectile, incident on a nucleus with some impact parameter  $b$ . The probability of transmission through the nucleus is simply

$$T = \exp(-z/\lambda), \quad \lambda = (\rho\sigma_T^{NN})^{-1}, \quad (2)$$

where  $z$  is the path length through the nucleus and is related geometrically to  $b$  and  $\rho$  is the nuclear density of the target. The total reaction cross section is then given by

$$\sigma_R = 2\pi \int b db [1 - \exp(-z/\lambda)]. \quad (3)$$

Equation (3) has been used by Ernst<sup>14</sup> to fit proton  $\sigma_R(E)$ .

Equation (3) is not very useful for projectiles other than single nucleons. However, it is possible to generalize to the case of a finite projectile

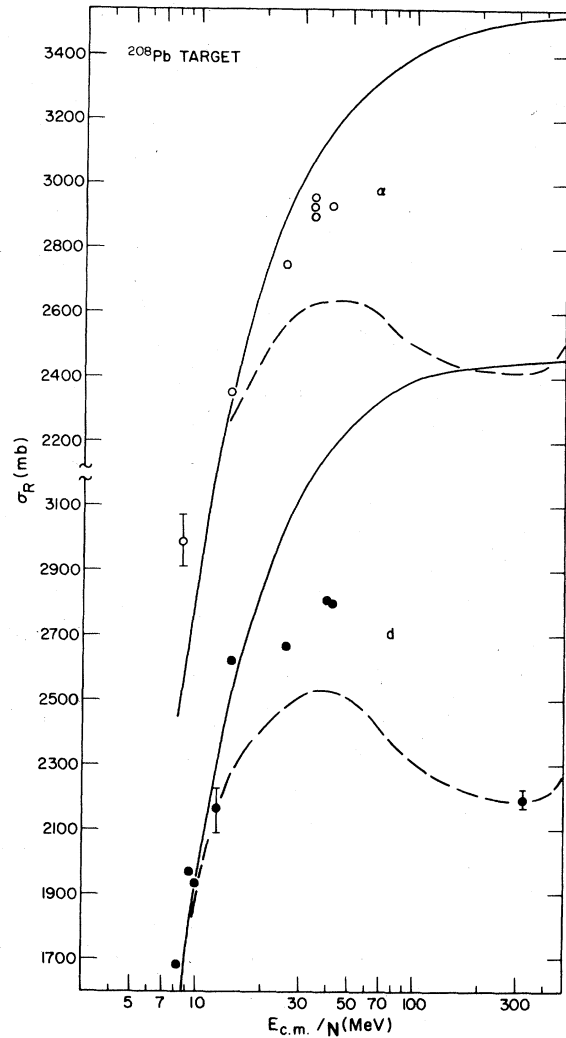


FIG. 6. Total reaction cross sections for a  $^{208}\text{Pb}$  target (see figure caption 4).

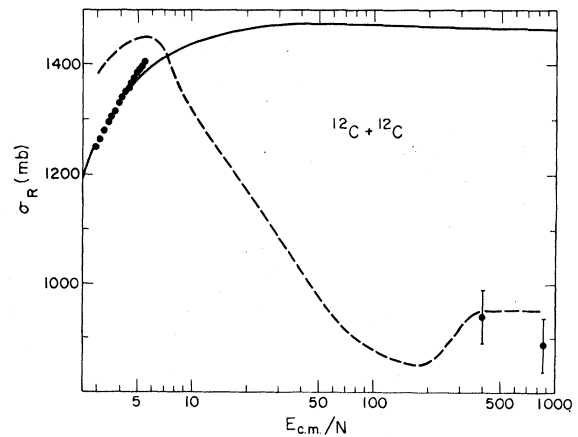


FIG. 7. Total reaction cross sections for the  $^{12}\text{C} + ^{12}\text{C}$  system (see figure caption 4).

by writing

$$\sigma_R = 2\pi \int b db [1 - \exp(-\sigma_T^{NN} \chi(b))] \quad (4)$$

$$\chi(b) = \int dr_1^2 \left[ \int dz_2 \rho_2(\bar{r}_1 - \bar{b} + z_2) \right. \\ \left. \times \int dz_1 \rho_1(\bar{r}_1 + z_1) \right], \quad (5)$$

where  $z_1$  and  $z_2$  are internal coordinates. This simple formulation of  $\sigma_R$  can also be derived from Glauber theory (e.g., the optical limit of Glauber theory).<sup>15</sup> We can apply a first order correction for Coulomb effects to these calculations by first calculating the classical distance of closest approach ( $b'$ ) for each asymptotic impact parameter ( $b$ ). In Eq. (4) we then use the  $\chi(b')$  which corresponds to the  $b$  value at each integration step. These Coulomb effects are important below about  $E_{c.m.}/N = 100$  MeV.

We are now ready to make predictions for the  $\pi$ - $\pi$   $\sigma_R(E)$ . These predictions are parameter free because electron scattering data<sup>11</sup> are used for  $\rho(r)$  and the experimental values, properly averaged over  $\sigma_T^{pp}$  and  $\sigma_T^{np}$  are used for  $\sigma_T^{NN}$ . Since the electron scattering charge distributions are not available for deuterons, we have used the analytical formulation of Humberston and Wallace<sup>16</sup> for the deuteron cases. The parameters for the density distributions of various nuclei used in the calculations are listed in Table II.

In Fig. 3, we display predictions for the experimental data on a  $^{12}\text{C}$  target discussed earlier. The predictions for all the projectiles on a  $^{12}\text{C}$  target are in rather impressive agreement with the experimental data at all energies even down to 10 MeV/ $N$ . As a check on our calculations we can compare our results, at the highest incident energies (where  $\sigma_T^{NN}$  is essentially constant) with the similar calculations of Barshay *et al.*<sup>17</sup> for the system  $\alpha + ^{12}\text{C}$ . Both calculation yield the same  $\sigma_R$  (560 mb). It should be noted that Chou and Yang<sup>18</sup> have used a similar concept to study high energy  $N$ - $N$  elastic scattering.

The agreement below 100 MeV/ $N$  is surprising, since Glauber theory is usually thought to break down at such low energies.<sup>19</sup> We note, however, that we have included Coulomb effects (to first order), and that previous, rather similar calculations by Bertini,<sup>20</sup> have successfully fitted proton-nucleus  $\sigma_R$  data down to 30 MeV.

Figures 4 through 6 display predictions for  $^{40}\text{Ca}$ ,  $^{90}\text{Zr}$ , and  $^{208}\text{Pb}$  targets. Again excellent quantitative agreement is obtained for all but the lowest incident energies. Our predictions for  $^{12}\text{C} + ^{12}\text{C}$  are shown in Fig. 7. Once again, good quantitative agreement is obtained with the (limited)

TABLE II. Nuclear densities.

Nucleus	$c$ (fm)	$z$ (fm)	$w$	Model
$^4\text{He}$	1.008	0.327	0.445	3PF <sup>a</sup>
$^{12}\text{C}$	2.355	0.5224	-0.149	3PF
$^{40}\text{Ca}$	3.669	0.5839	-0.1017	3PF
$^{90}\text{Zr}$	4.434	2.528	0.35	3PG <sup>b</sup>
$^{208}\text{Pb}$	6.624	0.549	0	3PF
$d^c$				
$^3\text{He}^d$				

$$^a \rho(r) = \rho_0(1 + wr^2/c^2) / \{1 + \exp[(r-c)/z]\}.$$

$$^b \rho(r) = \rho_0(1 + wr^2/c^2) / \{1 + \exp[(r^2 - c^2)/z^2]\}.$$

$$^c \rho(r) = \rho_0 \{ [u^2(2r) + w^2(2r)] / r^2 \} \text{ where}$$

$$u(r) = e^{-\alpha r} (1 - e^{-\delta(r-r_0)}) \sum_{i=1}^4 C_i e^{-(i-1)\mu r'},$$

$$w(r) = e^{-\alpha r} (1 - e^{-\rho(r-r_0)}) \left( 1 + \frac{3}{\alpha r} + \frac{3}{\alpha^2 r^2} \right) \sum_{i=1}^2 d_i e^{-(i-1)\mu r},$$

$$\mu = 0.7084 \text{ fm}^{-1}, \quad r_0 = 0.4842 \text{ fm}, \quad \alpha = 0.2317 \text{ fm},$$

$$\delta = 3.8 \text{ fm}^{-1}, \quad \rho = 0.8 \text{ fm}^{-1}, \quad c_1 = 0.8838 \text{ fm}^{-1/2},$$

$$c_2 = -0.0111 \text{ fm}^{-1/2}, \quad c_3 = -1.245 \text{ fm}^{-1/2},$$

$$c_4 = 0.3496 \text{ fm}^{-1/2},$$

$$d_1 = 0.02303 \text{ fm}^{-1/2}, \quad d_2 = -0.026605 \text{ fm}^{-1/2}.$$

$$^d \rho(r) = \rho_1(r) + \rho_2(r),$$

$$\rho_1(r) = \rho_0 \left[ \frac{1}{a^3} \exp(-r^2/4a^2) - \frac{c^2(6b^2 - r)^2}{4b} \exp(-r^2/4b^2) \right]$$

$$\rho_2(r) = A \rho_1(0) \left[ \frac{\sin(q_0 r)}{q_0 r} + \frac{p^2}{2q_0^2} \cos(q_0 r) \right] \exp\left(-\frac{p^2 r^2}{4}\right)$$

$$a = 0.675 \text{ fm}, \quad b = 0.836 \text{ fm}, \quad C = 0.366 \text{ fm},$$

$$A = -0.14, \quad p = 0.90 \text{ fm}^{-1}, \quad q_0 = 3.98 \text{ fm}^{-1}.$$

data.

The agreement between our calculations and the available experimental data strongly suggests that composite projectile and heavy-ion (at least  $^{12}\text{C} + ^{12}\text{C}$ ) collisions are dominated, at medium energies, by the simple  $N$ - $N$  interaction. The large energy dependence of the experimental  $\sigma_R(E)$  data for these systems suggests that heavy-ion collisions (or at least  $^{12}\text{C} + ^{12}\text{C}$ ) may not be dominated by bulk (e.g., collective, hydrodynamic) effects, which would yield a geometric  $\sigma_R$ . Such bulk effects might become more important with heavier projectiles. Thus  $\sigma_R(E)$  measurements may be capable of answering a fundamental question about heavy-ion collisions, i.e., to what extent are they dominated by  $N$ - $N$  collisions as opposed to hydrodynamic behavior.<sup>21</sup> Furthermore, the fact that  $\sigma_R$  falls below geo-

metric in the medium energy region might allow the observation of the onset of exotic effects in  $\pi$ - $\pi$  collisions, through a careful measurement of  $\sigma_R(E)$ . This possibility would not exist if  $\sigma_R$  were constant and geometric.

Equation (4) contains the quantity

$$1 - \exp(X) \text{ where } X = -\sigma_T^{NN} \chi(b). \quad (6)$$

This quantity may be thought of as one minus the transparency for a given impact parameter. Figures 8 and 9 plot this quantity as a function of impact parameter for the  $d + {}^{12}\text{C}$  and  ${}^{12}\text{C} + {}^{12}\text{C}$  systems. At low incident energies (large  $\sigma_T^{NN}$ ) there is no transparency until large distances are reached, thus the radius of the system is quite large justifying the notion that nucleus-nucleus collisions are strongly absorbing. However, at medium energies (small  $\sigma_T^{NN}$ ) the transparency is non-negligible at much smaller impact parameters. This leaves a considerable radial region, which is "translucent." This explains why nonzero  $T$  values are required at medium energies when the data are analyzed using Eq. (1). These results suggest that different radial regions are probed in low and medium energy  $\pi$ - $\pi$  collisions. The ability to probe the  $\pi$ - $\pi$  system to markedly lower radii may have important implications for nuclear structure studies.

Our microscopic calculations allow us to realistically study density distributions in  $\pi$ - $\pi$  collisions. For a given impact parameter ( $b$ ) we may plot the (electron scattering) densities, displaced from each other by  $b$ , and add them at the corresponding radii to obtain the resulting sum density along the line connecting the two centers. The probability of having both ions intact and unexcited at given  $b$  may be estimated using a plot like those shown in Figs. 8 and 9. This procedure is illustrated for  $\alpha + {}^{12}\text{C}$  with  $\sigma_T^{NN} = 30$  mb ( $E_i/N = 200$ – $300$  MeV) for two different impact parameters in Figs. 10 and 11. Notice that only low sum densities are achieved, at  $b = 3.5$  fm.

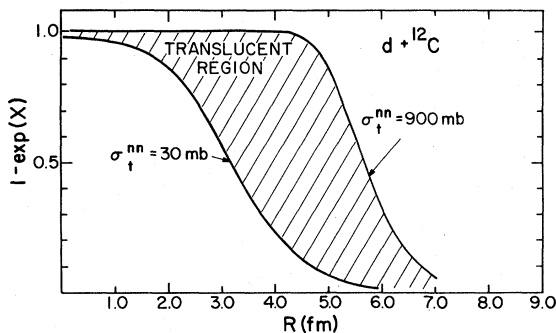


FIG. 8. The quantity  $1 - \exp(X)$  vs impact parameter for the  $d + {}^{12}\text{C}$  system.

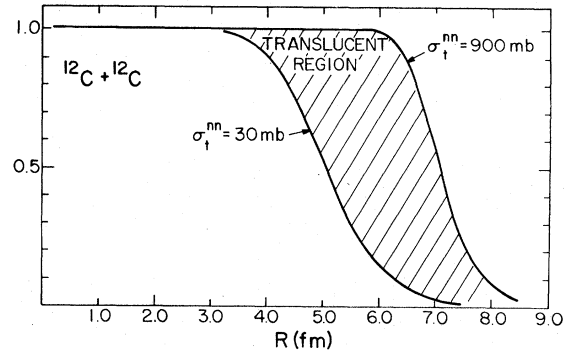


FIG. 9. The quantity  $1 - \exp(X)$  vs impact parameter for the  ${}^{12}\text{C} + {}^{12}\text{C}$  system.

At  $b = 2.5$  fm, densities are obtained which are significantly higher than normal. Since  $1 - \exp(X)$  is still 6.5%, there is a reasonable chance of reaching these conditions. It is not clear, how-

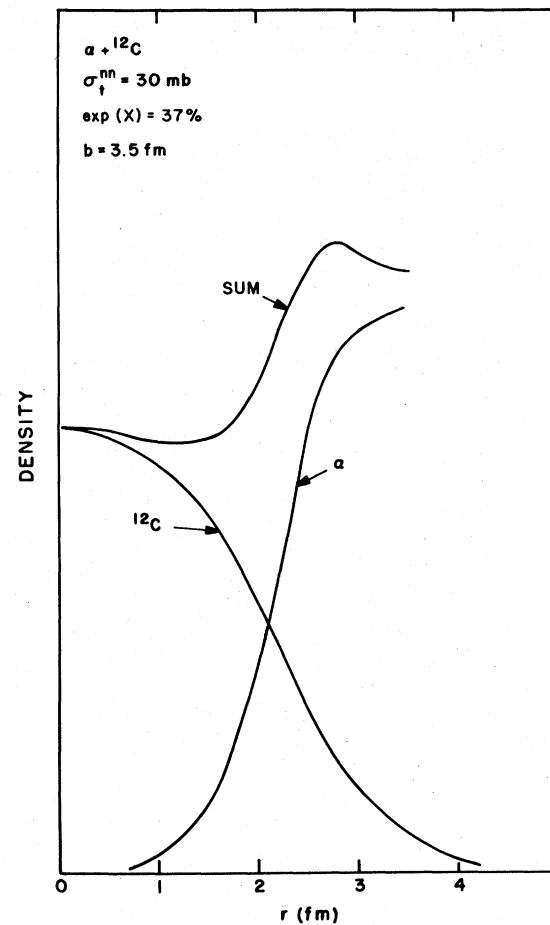
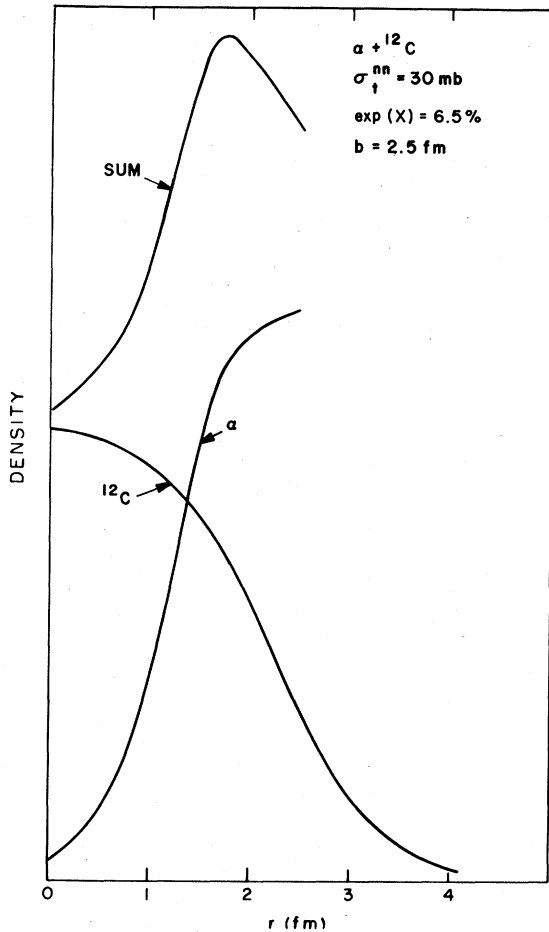
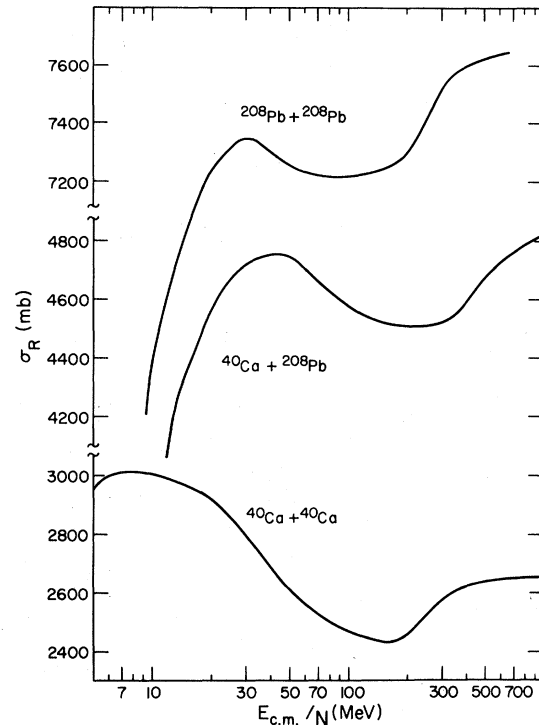


FIG. 10. Densities for the  $\alpha + {}^{12}\text{C}$  system for an impact parameter of 3.5 fm. The  ${}^{12}\text{C}$  ion is centered at  $r = 0$  while the  $\alpha$  nucleus is centered at  $r = 3.5$  fm (i.e., the impact parameter).

FIG. 11. Same as Fig. 12 except  $b = 2.5$  fm.

ever, that such low  $\sigma_T^{NN}$  values are conducive to exotic compressional effects, but our calculations, at least, serve as believable indicators of how/when higher than normal densities can be achieved.

We can extend our microscopic predictions to even heavier  $\pi$ - $\pi$  systems for which there is currently no experimental data. Figure 12 displays predictions for  $^{40}\text{Ca} + ^{40}\text{Ca}$ ,  $^{40}\text{Ca} + ^{208}\text{Pb}$ , and  $^{208}\text{Pb} + ^{208}\text{Pb}$  systems. Notice that the characteristic  $N$ - $N$  dip is still predicted even for these very heavy systems. The overall shape is somewhat different than for lighter systems because of the higher Coulomb barrier. Table I lists the geometric cross sections for these cases. The medium energy  $\sigma_R$  values predicted by our microscopic calculations exceed the geometric values at energies above 50 MeV/ $N$ , even in the dip region. The origin of this effect is easy to understand. The tail of the nuclear density sticks out beyond the equivalent sharp cutoff radius. Thus the large size of the nuclei involved yields a considerable path length as the projectile moves past

FIG. 12. Microscopic predictions for heavier  $N$ - $N$  systems.

the target through this nuclear density tail. Therefore,  $\sigma_R$  can exceed the value given by the geometrical limit obtained from the (electron scattering derived) sharp cutoff radius. This result suggests that for heavy  $\pi$ - $\pi$  systems, as well as for composite projectile  $\pi$ - $\pi$  systems, the concept of a geometrical  $\sigma_R$  is not very meaningful.

Finally we discuss some of the effects which are neglected in our microscopic calculations. Equations (4) and (5) predict  $\sigma_R$  assuming that there exist no internal interaction or motion of the nucleons in either the target or projectile. One should, however, include Fermi motion and Pauli blocking in the calculations. These effects have been shown<sup>22</sup> to effectively reduce  $\sigma_T^{NN}$  at low energies. Thus  $\sigma_R$  would decrease if Fermi motion and Pauli blocking were included. We are also neglecting the influence of the  $\pi$ - $\pi$  nuclear interaction on the trajectories of the projectile. At low energies the real  $\pi$ - $\pi$  interaction is sufficiently strong to appreciably pull the projectile and target together. This would cause  $\sigma_R$  to increase. These two effects are probably the largest corrections to be applied to Eqs. (4) and (5), but would be expected to be most important at the lower energies ( $E/N \leq 50$  MeV). Notice that the signs of the two effects are opposite, which may explain why our simple predictions fit

the experimental data so well, even at low energies. Another effect which is not explicitly included in our calculations is the coherent excitation of collective states by the Coulomb or real nuclear potentials.

### V. CONCLUSIONS

Using the rather limited amount of available experimental data, we find that  $\sigma_R(E)$  for composite projectiles displays an energy dependence, which is as strong or stronger than that for protons. Specifically,  $\sigma_R$  is not geometric in the energy region  $50 < E_i/N < 600$  MeV. These effects apparently stem from the strong energy dependence of  $\sigma_N^{TT}$ . Microscopic (based only on  $\sigma_N^{TT}$  and electron scattering densities) model calculations are capable of reproducing all the features of the data including quantitative agreement in the energy region  $E_i/N > 20$  MeV. These results emphasize the dominance of the  $N$ - $N$  inter-

action in all of the  $\pi$ - $\pi$  collisions for which we have data. These results are rather unexpected and are likely to have important implications for medium energy composite projectile and heavy-ion physics. For example, the excellent agreement between our (parameter free) microscopic calculations and the available experimental data suggests that medium energy heavy-ion projectiles behave like bags of noninteracting nucleons. Thus collective or hydrodynamic effects are highly suppressed. Because of the present sparsity of data, our results are rather controversial suggesting that a larger number of experimental measurements are needed.

### ACKNOWLEDGMENTS

We have been assisted and encouraged in this study by J. Cramer, J. Friar, J. Ginocchio, L. Ray, R. Stokstad, and J. Shepard. This work was supported by the DOE-DMA.

- <sup>1</sup>W. Hess, *Rev. Mod. Phys.* **30**, 365 (1958); O. Benary *et al.*, UCRL-20000 NN, unpublished.
- <sup>2</sup>P. Renberg *et al.*, *Nucl. Phys.* **A183**, 81 (1972). It appears that  $\sigma_R = \pi(R + \lambda)^2(1 - zZe^2/RE)(1 - T)$  should be the correct formula to use; however, very similar results are obtained by both equations.
- <sup>3</sup>The sources of the data in Fig. 2 are listed in R. DeVries and J. Peng, *Phys. Rev. Lett.* **43**, 1373 (1979).
- <sup>4</sup>J. Blair, in *Lectures in Theoretical Physics*, edited by W. E. Brittin *et al.*, Vol. VIII C, p. 343 (University of Colorado Press, Boulder, Colorado, 1966).
- <sup>5</sup>D. Goldberg, S. Smith, and G. Burdzik, *Phys. Rev. C* **10**, 1362 (1974).
- <sup>6</sup>G. Alkhozov *et al.*, *Nucl. Phys.* **A280**, 365 (1977).
- <sup>7</sup>S. Mayo, W. Schimmerling, M. Sametband, and R. Eisberg, *Nucl. Phys.* **62**, 393 (1965); R. Balcarcel and J. Griffith, *Phys. Lett.* **26B**, 213 (1968); R. DeVries, J. Lilley, and M. Franey, *Phys. Rev. Lett.* **37**, 481 (1976).
- <sup>8</sup>G. Duhamel *et al.*, *Nucl. Phys.* **A174**, 485 (1971); F. Hinterberger *et al.*, *ibid.* **A111**, 265 (1968); O. Aspelund *et al.*, *ibid.* **A253**, 263 (1975); C. Busch, T. Clegg, S. Datta, and E. Ludwig, *ibid.* **A223**, 183 (1974); G. Perrin *et al.*, *ibid.* **A193**, 215 (1972); E. Auld *et al.*, *ibid.* **A101**, 65 (1967); E. Newman, L. Becker, B. Freedom, and J. Hiebert, *ibid.* **A100**, 225 (1967); D. Goldberg, private communication; T. Sawada, *Nucl. Phys.* **74**, 289 (1965); H. Guratzsch, G. Hofmann, H. Muller, and G. Stiller, *Nucl. Phys.* **A140**, 129 (1970).
- <sup>9</sup>See Ref. 7 and J. Jafar *et al.*, *Nuovo Cimento* **48A**, 165 (1967); L. Dutton *et al.*, *Phys. Lett.* **16**, 331 (1965).
- <sup>10</sup>J. Jaros *et al.*, *Phys. Rev. C* **18**, 2273 (1978).
- <sup>11</sup>C. W. DeJager, H. DeVries, and C. DeVries, *At. Data Nucl. Data Tables* **14**, 479 (1974).
- <sup>12</sup>N. Willis *et al.*, *Nucl. Phys.* **A204**, 454 (1973); P. Gailard *et al.*, *ibid.* **A131**, 353 (1969); G. Hauser *et al.*, *ibid.* **A182**, 1 (1972); G. Hauser *et al.*, *ibid.* **A128**, 81 (1969); H. Apell *et al.*, *ibid.* **A246**, 477 (1975); H. Chang *et al.*, *ibid.* **A270**, 413 (1976); B. Tatischeff and I. Brissand, *ibid.* **A155**, 89 (1970); N. Baron, R. Leonard, and W. Stewart, *Phys. Rev. C* **4**, 1159 (1971); S. Smith *et al.*, *Nucl. Phys.* **A207**, 273 (1973); L. Bimbot *et al.*, *ibid.* **A210**, 397 (1973); D. Goldberg *et al.*, *Phys. Rev. C* **7**, 1938 (1973); G. Igo and B. Wilkins, *Phys. Rev.* **131**, 1251 (1963); F. Cecil and R. Peterson, *Phys. Lett.* **56B**, 335 (1975); M. Fawzi, *Z. Phys.* **250**, 120 (1972); J. Vidal *et al.*, *J. Phys. (Paris) C* **1**, 128 (1966); S. Wiktor *et al.* and A. Djalois *et al.*, *Julich Annual report* (1976), unpublished; L. Put and A. Paans, *Phys. Lett.* **49B**, 266 (1974); C. Bingham, M. Halbert, and R. Bassel, *Phys. Rev.* **148**, 1174 (1966); R. Tickle and W. Gray, *Nucl. Phys.* **A247**, 187 (1975); O. Hansen, T. Belote, and W. Dorbenbusch, *ibid.* **A118**, 41 (1968); M. Gaillard *et al.*, *ibid.* **A119**, 161 (1968); J. Burq, G. Hadinger, J. Kouloudjian, and J. Meyer, *ibid.* **A149**, 488 (1970); W. Fitz, J. Heger, R. Santo, and S. Wenneis, *ibid.* **A143**, 113 (1970); R. Roche *et al.*, *ibid.* **A220**, 381 (1974); H. Burgi *et al.*, *ibid.* **A247**, 322 (1975); F. Baker, S. Davis, C. Glashauser, and A. Robbins, *ibid.* **A250**, 79 (1975); L. Knutson and W. Haerberli, *Phys. Rev. C* **12**, 1469 (1975); D. Kovar, N. Stein, and C. Bockelman, *Nucl. Phys.* **A231**, 266 (1974); A. Jeans *et al.*, *ibid.* **A128**, 224 (1969); J. Childs, W. Daehnick, and M. Spisak, *Phys. Rev. C* **10**, 217 (1974); J. Bojowald *et al.*, *Julich Annual report* (1977), unpublished; J. Jafar *et al.*, *Nucl. Phys.* **A161**, 105 (1971); W. Burcham *et al.*, *ibid.* **A246**, 269 (1975); T. Fujisawa *et al.*, *J. Phys. Soc. Jpn.* **34**, 5 (1972); R. Singh *et al.*, *Nucl. Phys.* **A205**, 97 (1973); G. Ball and J. Cerny, *Phys. Rev.* **177**, 1466 (1969); G. Ronsin, M. Vergnes, G. Rotbard, and J. Kalifa, *Nucl. Phys.* **A207**, 353 (1973); D. Youngblood, R. Kozub, R. Kenefick, and J. Hiebert, *Phys. Rev. C* **2**, 477 (1970); H. Chang, thesis, 1975 (J. Shepard, private communication);

- P. Urone, L. Put, H. Chang, and B. Ridley, Nucl. Phys. A163, 225 (1971); H. Morsch and R. Santo, *ibid.* A179, 401 (1972); J. Rapaport, W. Dorenbusch, and T. Belote, *ibid.* A177, 307 (1971); J. Luetzelschwab and J. Hafele, Phys. Rev. 180, 1023 (1969); J. Yntema, B. Zeidman, and R. Bassel, Phys. Lett. 11, 302 (1964); D. Rundquist, M. Brussel, and A. Yavin, Phys. Rev. 168, 1287 (1968); E. Gibson *et al.*, *ibid.* 155, 1194 (1967); P. Urone, L. Put, B. Ridley, and G. Jones, Nucl. Phys. A167, 383 (1971); N. Nakanishi, Y. Chiba, Y. Awaya, and K. Matsuda, *ibid.* A140, 417 (1970); also see Refs. 5–10.
- <sup>13</sup>R. Stokstad *et al.*, Phys. Rev. C 20, 655 (1979).
- <sup>14</sup>D. Ernst, Phys. Rev. C 19, 896 (1979).
- <sup>15</sup>W. Czyz and L. Maximon, Ann. Phys. (N.Y.) 52, 59 (1969).
- <sup>16</sup>J. Humberston and J. Wallace, Nucl. Phys. A141, 362 (1970).
- <sup>17</sup>S. Barshay, C. Dover, and J. Vary, Phys. Rev. C 11, 360 (1975).
- <sup>18</sup>T. Chou and C. Yang in *High Energy Physics and Nuclear Structure*, edited by G. Alexander (North-Holland, Amsterdam, 1967).
- <sup>19</sup>P. Schwaller *et al.*, Nucl. Phys. A316, 317 (1979); L. Ray, Phys. Rev. C 20, 1857 (1979).
- <sup>20</sup>H. Bertini, Phys. Rev. C 5, 2118 (1973).
- <sup>21</sup>A. Amsden *et al.*, Phys. Rev. Lett. 38, 1055 (1977).
- <sup>22</sup>D. Saloner and C. Teopffer, Nucl. Phys. A283, 131 (1977).